Presented at Symposium F, "Microcrystalline & Nanocrystalline Semiconductors," Materials Research Soc., Fall, 1998 (Boston, MA)

OPTICAL ANALYSIS OF PLASMA ENHANCED CRYSTALLIZATION OF AMORPHOUS SILICON FILMS

L. MONTÈS*, L. TSYBESKOV**, P.M. FAUCHET**, K. PANGAL***, J.C. STURM***, S. WAGNER***,
* Laboratoire de Spectrométrie Physique, CNRS (UMR 5588), 38402 Saint-Martin d'Hères Cedex, France, Laurent.MONTES@ujf-grenoble.fr
** ECE Department, University of Rochester, Rochester, NY 14627.
*** ECE Department, Princeton University, Princeton, NJ 08544.

ABSTRACT

Low-temperature crystallization of a-Si is important for display and Silicon-On-Insulator (SOI) technologies. We present optical characterization (Raman scattering and photoluminescence) of H_2 and O_2 plasma enhanced crystallization of a-Si:H films. H_2 plasma treatment is shown to be the most efficient, leading to larger grain sizes, and both H_2 and O_2 plasma lead to visible photoluminescence (PL). Recently, the PL of re-crystallized a-Si films has been explained in terms of quantum confinement [1]. The mean size of the crystallites in our re-crystallized films is determined by Raman scattering for different treatments parameters. No correlation between size and the photon energy of the visible emission is found. However, we can clearly distinguish between the PL from purely amorphous and re-crystallized a-Si:H films : Their PL temperature dependence and spectra are very different. The origin of the visible PL in re-crystallized thin Si films is discussed.

INTRODUCTION

Silicon nanocrystals (nc-Si) with sizes in the order of the nanometer are now elaborated using different fabrication techniques [1-7]. For silicon grains with size below 10 nm, the quantum size effects emerge as their size is comparable to the diameter of the bulk exciton 4-5 nm, which results in a widening of the band gap and a collateral increase of the probability for optical transitions that can be useful for optoelectronic applications. Porous silicon has been widely studied for its luminescent properties at room temperature in the visible [2,3], yet the mechanism contributing to the emission is still uncertain. In comparison with porous silicon, re-crystallized a-Si:H films are more stable and can be deposited over large area glass substrates, therefore they are of potential use in thin solar cells, as active layers in thin film transistors arrays for flat panel displays, with a better conduction than polycrystalline device. However the origin of the PL in these films is not well known but is of significance to contribute to a better control of the structures in order to increase the efficiency and the stability of the emitting material. Different mechanisms for excitation and radiative recombination are suggested, based on quantum confinement (excitation between the quantized levels inside the nanocrystallites) [1,4], on spatial confinement [3], and luminescent compounds or defect states [5]. Liu et al [1] reported the room-temperature photoluminescence of nc-Si crystals embedded in a large fraction of amorphous tissue, and proposed quantum confinement to be responsible for the PL peak position.

To address the origin of the light emission, a comparative study of samples with different sizes are analyzed through Raman scattering and PL temperature dependence to uncover the relation, if any exists, between the size of the crystals and the photoluminescence.

Mat. Res. Soc. Symp. Proc. Vol. 536 © 1999 Materials Research Society

EXPERIMENT

Hydrogenated amorphous silicon films (a-Si:H) were deposited by PECVD using pure silane, on 7059 glass substrates at substrate temperature T_s of 150°C (set A) and 250°C (set B), and RF power ~5 W. A subsequent RF plasma exposure was realized in a parallel plate Reactive Ion Etcher (RIE) at room temperature with hydrogen or oxygen. Annealing in a furnace at 600°C in N_2 for 3 hours was completed to obtain the re-crystallized samples, using UV reflectance to monitor the crystallization process. The thickness of the film varied from 110 to 180 nm.

The Raman spectra of the transverse optical (TO) mode of the material were acquired with a Jobin Yvon U1000 instrument by exciting the sample with the 514.5 nm line of an Ar^+ laser. The power on the sample was of about 1 mW and the light was collected trough a microscope in the backscattering configuration. For the photoluminescence acquisition, visible emission was detected though a conventional optical multichannel analyzer set-up, while the infra-red region was detected with a North Cost high purity germanium detector.

RESULTS AND DISCUSSION

Raman analysis

The Raman spectrum of a crystalline silicon reference sample is dominated by a sharp lorentzian feature centered at 520 cm^{-1}, with a measured width at half maximum of 4 cm^{-1}. The feature corresponding to a-Si:H has a gaussian shape centered at 480 cm^{-1}, broad because the momentum conservation rule is relaxed by structural disorder. The Raman spectra of all the studied samples presented amorphous bands, while only the re-crystallized ones presented an additional TO-like silicon crystalline band. An example of spectrum is shown in Fig. 1 where both contributions clearly appears.

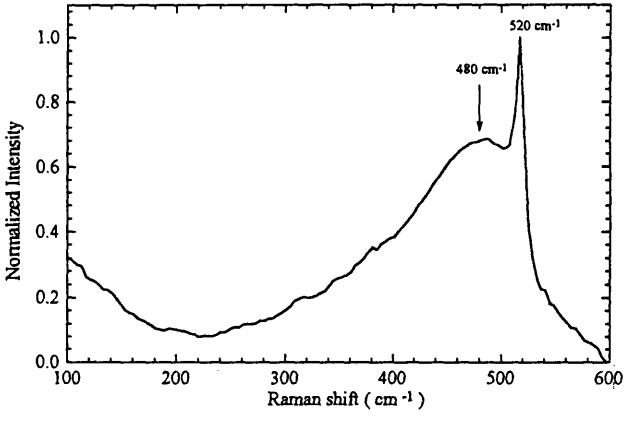

Fig. 1 : Raman spectra after re-crystallization for sample B2 (growth temperature Ts=150°C and hydrogen plasma treatment) : both a-Si:H and nc-Si TO-lines are present.

The crystalline band in our samples is highly asymmetric in the low frequency side, which is a clear indication of the stress of the structure. As the mean crystallite size decreases, the Raman peak broadens and shifts to lower frequency. The Raman spectra in the nc-Si peak region is represented in Fig. 2 for several treated samples.

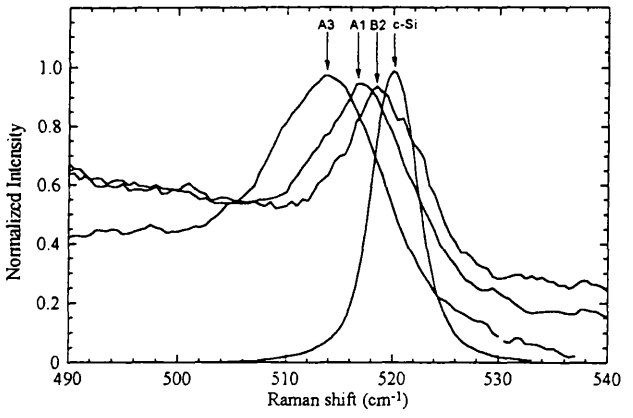

Fig. 2 : Raman shift TO line of re-crystallized samples A1, A3, B2 (see Table 1 for details) with comparison to bulk crystalline silicon as reference.

The correlation length of the nc-Si crystallites was deduced from a fitting with lorentzian curves and comparison with the values calculated by Fauchet [8], assuming a spherical shape of the grains. The resulting values of the peak shift $\Delta\omega$ and width are represented in Fig. 3 for the re-crystallized samples, leading to estimated sizes varying from 5 to 10nm, so that quantum size effects might be expected for these films.

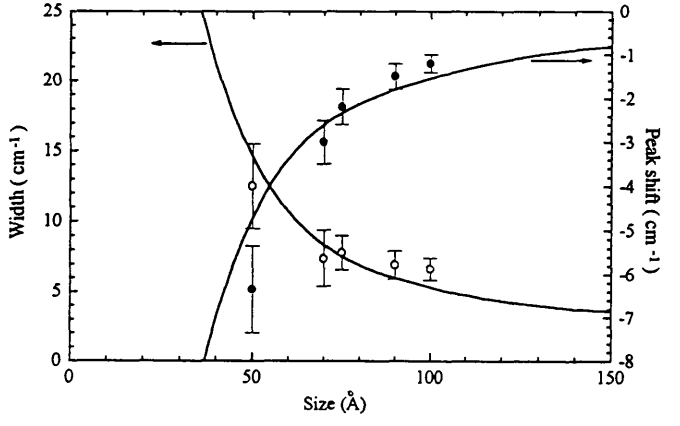

Fig. 3 : Size determination from width and peak shift of the Raman spectra for the re-crystallized samples (from left to right : A3, B1, A2, B3, B2) with comparison to [8].

The mean grain size d can also be deduced from Fig. 1 using the formula :

$$d = 2\pi\sqrt{\frac{B}{\Delta\omega}} \quad \text{with B=3 nm}^2\text{.cm}^{-1} \qquad (1)$$

The volume fraction of nanocrystallites is defined by $X_c=I_c/(Ic+yI_a)$ [9], where y is the ratio of the Raman cross section of the TO mode of crystalline and amorphous, I_c is the crystalline component of the Raman spectra and I_a is the amorphous component.
The scattering factor y can be obtain with the formula [9]:

$$y(d) = 0.1 + e^{-(d/250)} \qquad (2)$$

We find sizes d of the crystallites range from 5 to 10 nm in good agreement with our previous plot and a volume ratio of crystalline in the order of 55% for almost all the re-crystallized samples is obtained. The results for the nc-Si samples are reported in Table 1.

Table 1 : nc-Si samples : growth temperature of amorphous film (Ts), plasma treatment before re-crystallization, mean size d and crystalline fraction Xc from Raman spectra, PL peak wavelength at room temperature, characteristic temperature T_0 and energy shift with temperature.

Sample	T_s (°C)	Plasma Treatment	Mean size (Å)	Xc (%)	PL (nm)	PL (eV)	T_0 (K)	$\Delta E/\Delta T$ ($meV.K^{-1}$)
A3	150°C	O_2	50	60	803	1.54	64	-0.04
A1	150°C	-	70	55	780	1.59	65	-0.05
B1	250°C	-	70	54	804	1.54	33	-0.13
A2	150°C	H_2	75	54	802	1.54	69	-0.04
B3	250°C	O_2	90	54	737	1.68	42	-0.06
B2	250°C	H_2	100	54	660	1.88	34	-0.12

The effect of the plasma treatment before annealing differs depending on the element (hydrogen or oxygen) and the temperature of the substrate T_s during the deposition. With increasing T_s, the effect of the plasma treatment is more perceptible, as it increases the size of the grains, while the crystalline fraction in the films remains almost constant. Hydrogen plasma is obviously the most efficient, as size is increased from 70Å to 100Å, for T_s = 250°C. On the contrary the oxygen plasma treatment for low T_s has a tendency to decrease the mean diameter of the grain while increasing the volume fraction. The fitting of sample A3 in Fig. 3 is unsatisfactory as the width of the Raman line is especially reduced for this size : this is an indication of the stress of the material and is probably correlated with the high volume ratio. The nucleation sites are more distributed in the film, leading to numerous nucleation of smaller crystallites. Higher defects density in the structure may also explain this result, because the temperature T_s corresponding is low and consequently the quality of a-Si:H is affected. Moreover, the presence of defects within the grains can confine the phonons, resulting in smaller correlation length (higher shifts) than the actual grain size. Compared to oxygen (or argon) plasma, hydrogen plasma has the largest effect on grain size, with the crystallization time reduced by a factor of five relative to non-plasma treated samples [7].

Photoluminescence and temperature dependence

Visible PL is obtained for plasma treated samples, persisting even at room temperature for the re-crystallized ones. In the later case, PL was stable over 6 months and no fatigue was observed.

An increase of hydrogen or oxygen content due to the plasma treatment leads to a widening of the band gap and increases the PL quantum efficiency when no crystallization is

done. The PL peak energy is blue shifted (1.5eV) relative to the low-temperature PL in the near infrared region of standard a-Si:H films, while the temperature dependence parameters are very close to those of a-Si:H (see Fig. 4).

The values of the PL peak position at room temperature are reported in Table 1 for the re-crystallized films. No size correlation can be deduced from our data : this disconnection eradicates any quantum size effect related phenomenon. The PL temperature dependence was studied to investigate the mechanism involved in the recombination process. In standard a-Si:H films, for temperatures higher than a critical temperature T_c (50-100K for our samples), the recombination process is dominated by the dissociation of electron-hole pairs by thermal activation and non-radiative recombination through defects, which results in the quenching of the PL. Although the parameters are different, we observed PL dependency similar to that of a-Si:H : the temperature quenching of PL follows an exponential decrease with temperature,

$$\frac{I(T)}{I_0} = e^{-\frac{T}{T_0}} \qquad (3)$$

where I_0 is the maximum photoluminescence intensity (corresponding to T_c), and T_0 is a characteristic temperature (~23K for a-Si:H [10]). This ratio is related to the probability of radiative and non-radiative recombination, respectively W_r and W_{nr},

$$\frac{I(T)}{I_0} = \frac{W_r}{W_{nr} + W_{nr}} \qquad (4)$$

Thus Fig. 4 is a plot showing the dependence $\ln(W_{nr}/W_r)=\exp(T/T_0)$ versus T, from which T_0 can be extracted. From Table 1 it is clear that T_0 is strongly dependent on the growth temperature parameter T_s : lower deposition temperature corresponds to higher T_0 values. According to the luminescence model of band-tail states proposed by Street [11], T_0 in a-Si:H is proportional to the width of exponential band tail states. High T_0 values corresponds to deeper extending of the band tail states towards the middle band gap with a less pronounced slope of the exponential decay in the density of states, which reflects an increase of the disorder in the material and a weaker temperature dependence of the PL quenching. Changes in the structure due to the lattice mismatch between the amorphous and crystalline phases, together with

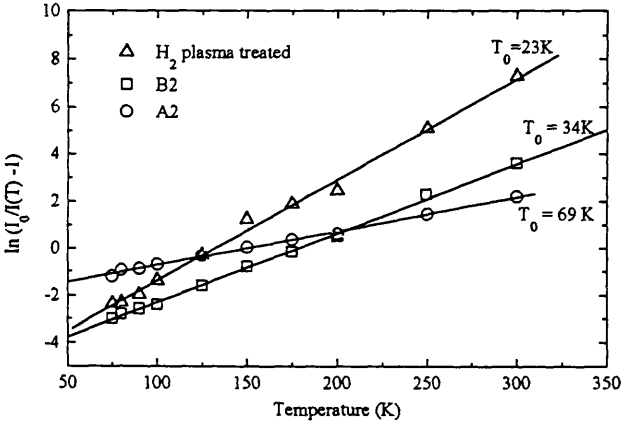

Fig. 4 : PL temperature dependence of for samples A2, B2 and a H_2 plasma treated film without re-crystallization.

abundant hydrogen or oxygen concentration induced by plasma treatment is responsible for those high T_0 values. With increasing temperature, carriers trapped in the band tail states move towards the middle of the band gap, leading to a redshift of the PL peak, as suggested by Street et al. [11]. This shift $\Delta E/\Delta T$ is found to be insignificant for our samples (in the order of $10^{-5}eV.K^{-1}$ instead of $10^{-3}eV.K^{-1}$ for a-Si:H). The weak temperature dependence of luminescence can be interpreted in terms of passivation due to the reduction of the density of mid-gap defects. As a consequence a PL signal is still efficient at room temperature.

CONCLUSIONS

Hydrogen plasma treatment reveals the important role of hydrogen in re-crystallization of a-Si:H films, with an enhancement of the nucleation rate leading to larger grain sizes. Comparison of the different crystallite sizes, with an almost constant crystalline fraction in the films, exclude any correlation between the size of the crystals and the PL wavelength that was observed : the luminescence has no relation with quantum size effect. Plasma treatment lead to PL with the temperature dependence parameters characteristic of standard a-Si:H films, while re-crystallization processes weaken this dependence. The temperature quenching of the PL is diminished and visible light emission is maintained even at room temperature.

REFERENCES

1. S. Tong, X.-n. Liu, and X.-m. Bao, Appl. Phys. Lett. **66** (4), 469 (1995); S. Tong, X.-n. Liu, T. Gao, X-m Bao, Y. Chang, W-z Shen and W.-g. Tang, Solid State Commun. **104** (10), 603 (1997).
2. L.T. Canham, Appl. Phys. Lett. **57** (10), 1046 (1990)
3. I. Solomon, R.B. Wehrspohn, J.-N. Chazalviel, F. Ozanam, J. Non-crystalline Solids **227-230**, 248. (1998); M.J. Estes and G. Moddel, Appl. Phys. Lett. **68** (13), 1814 (1996).
4. E. Bustarret, E. Sauvain, and M. Rosenbauer, Thin Solid Films **276**(1/2), 134 (1996).
5. K. Luterová, P. Knápek, J. Stuchlík, J. Kocka, A. Poruba, J. Kudrna, P. Malý, J. Valenta, J. Dian, B. Hönerlage, I. Pelant, J. Non-crystalline Solids, **227-230**, 254 (1998).
6. D.J. Lockwood,, Z.-H. Lu, and J.M. Baribeau, Phys. Rev. Letters **76** (3), 539 (1996); L. Tsybeskov , G.F. Grom, K.D. Hirshman, L. Montès, and P.M. Fauchet, T.N. Blanton, J.P. McCaffrey, J.M. Baribeau, G.I. Sproulc, H.J. Labbé and D.J. Lockwood, MRS Fall Meeting 1998 (Symp. F)
7. K. Pangal, J.C. Sturm and S. Wagner, Proc. Symp. Mat. Res. Soc. **507** (1998) (to be published)
8. P.M. Fauchet, *Light Scattering in Semiconductors Structures and Superlattices*, edited by D.J. Lockwood and J.F. Young, (Plenum Press, New York, 1991), p.229
9. R. Tsu, J. Gonzalez-Hernandez, S.S. Chao, S.C. Lee, and K. Tanaka, Appl. Phys. Lett. **40**, 534 (1982); E. Bustarret and M.A. Hachicha, M. Brunel, Appl. Phys. Lett. **52** (20), 1675 (1988)
10. R.W. Collins, M.A. Paesler and W. Paul, Solid State Commun. **34**: (10), 833 (1980)
11. R.A. Street, *Semiconductors and Semimetals*, Vol. 21B, edited by J.I. Pankove (Academic Press, Orlando, 1984), p.197